METHOD OF ANALYSIS OF SOME MICROWAVE PLANAR NETWORKS

Reza Mehran
Institut für Allgemeine und Theoretische Elektrotechnik, GHD
Department of Electrical Engineering, University Duisburg
Bismarckstrasse 81
41 Duisburg, Fed.Rep. of Germany

ABSTRACT

A method of analysis of some planar microwave structures is presented. It is shown that the frequency dependent scattering parameters of more complex structures can be given by simple formulas, which contain the frequency dependent scattering parameters of discontinuities and junctions. The filtering properties of ring-filters are investigated in detail.

INTRODUCTION

In the last years, the frequency dependent properties of a variety of microstrip discontinuities (Fig.1) have been analysed, using a waveguide model (Fig.1a). In this model, which is described in many studies, the fringing effects as well as the dispersion effects are considerd by ascribing to the line frequency dependent effective width $w_{eff}(f)$ and effective permittivity $\varepsilon_{eff}(f)$ [1,2]. The comparison of the theoretical results with the associated measurements shows:

1. The parasitic effects caused by higher order modes when calculating the dominant mode scattering matrix of microstrip discontinuities can be efficiently described by the waveguide model.
2. Due to the fast convergence of the applied method of analysis the computation-time, needed to determine the S-matrix of the structures shown in Fig. 1 (which will be important in the optimization procedure) is not to high. In detail the computer-time on a Control Data Cyber 76 necessary for one frequency points amount 5 ... 100 ms.

An important advantage of the methode which has been applied to single discontinuities [1-6] consists in the fact that the results can be used to more complex structures with very small mathematical effort by simply combining the elements. This leads to a fast numerical computation of microstrip circuits, and shall be demonstrated by the calculation of the properties of two kinds of microstrip filter structures (Fig.2).

CALCULATION OF THE NETWORKS

For the computation of the first kind of microstrip filters shown in Figs. 2c, 2d the geometrical structure is subdivided into individual filter elements (Fig. 2a) and pure discontinuity elements (Fig. 1s) as well as line-sections. The frequency dependent scattering matrices of these elements operated as 2-ports are calculated considering loss, dispersion effects, parasitic inductive and capacitive effects in the discontinuities. These individual scattering matrices are converted into the corresponding cascade matrices and after multiplying them, finally the resulting cascade matrix is reconverted into a scattering matrix again. While the scattering parameters of discontinuities (Fig. 1) are known from the field-matching solution [1-6], the scattering parameters of the filter element shown in Fig. 2a must be obtained. Considering the frequency range, in which only the dominant mode can be propagate, the scattering parameters $s^F_{\nu\mu}$ of this filter element as a function of the scattering parameters $s^T_{\nu\mu B}$ of the T-junction with reference plane T_ν can easily be given by:

$$
\begin{aligned}
s^F_{11} &= S^T_{33B} + (s^T_{13B}.EX_5)^2/NB \ , \\
s^F_{22} &= s^T_{22B}.EX_4^2 + (s^T_{12B}.EX_4.EX_5)^2/NB \ , \\
s^F_{12} &= s^T_{23B}.EX_4^2 + s^T_{12B}.s^T_{13B}.EX_4.EX_5^2/NB \ , \\
NB &= 1/r_5 - s^T_{11B}.EX_5^2 \ , \quad EX_\nu = EXP(-j\beta_\nu l_\nu) \ .
\end{aligned}
\tag{1}
$$

Because the width of the rings of the second kind of microstrip filters (Figs. 2e, 2f), in general, is much smaller than the circumference, the anular structures can be considered as a connection of T-junctions and line-sections. Using the symmetrical properties and reciprocity theorem, it can be shown that the calculation of the network filter (Fig. 2f) can be reduced to the computation of the microstrip structure given in Fig. 2b. Applying the theory of linear networks the scattering parameters $s^{FR}_{\nu\mu}$ of the considered network are then related to the scattering parameters $s^T_{\nu\mu}$ of the T-junctions and line length l_ν as follows:

$$
\begin{aligned}
s^{FR}_{11} &= (T^0_{11}+T^S_{11})/2 \ , \quad s^{FR}_{12} = (T^0_{11}-T^S_{11})/2 \ , \\
s^{FR}_{13} &= (T^0_{13}+T^S_{13})/2 \ , \quad s^{FR}_{14} = (T^0_{13}-T^S_{13})/2 \ , \\
T^0_{11} &= (r^0_{10}+r^S_{1S})/2 \ , \quad T^S_{11} = (r^S_{10}+r^S_{1S})/2 \ , \\
T^0_{13} &= (r^0_{10}-r^0_{1S})/2 \ , \quad r^S_{13} = (r^S_{10}-r^S_{1S})/2 \ ,
\end{aligned}
$$

and $r_1=s^T_{11A}+s^T_{13A}.EX_3.A_{13}+s^T_{12A}.EX_2.A_{23}$,

$$A_{11}=1/r_3-s^T_{33A}.EX_3^2 \quad , \quad A_{22}=1/r_2-s^T_{22A}.EX_2^2 \quad ,$$

$$A_{12}=-s^T_{23A}.EX_2.EX_3 \quad , \quad NA=A_{12}^2-A_{11}A_{22}, \qquad (2)$$

$$A_{23}=(A_{12}.s^T_{13A}.EX_3-A_{11}.s^T_{12A}.EX_2)/NA \ ,$$

$$A_{13}=(A_{12}.s^T_{12A}.EX_2-A_{22}s^T_{13A}.EX_3)/NA \ .$$

For r_3 it is worth:

$$r_3=s^F_{11}+s^{F^2}_{12}/(1/r_4-s^F_{22}) \ .$$

In the above expressions (1) and (2) it must be taken into account:

$r_2=r_4=+1$ or $r_5=+1$ for the upper index or lower index 0 respectivly,

$r_2=r_4=-1$ or $r_5=-1$ for the upper index or lower index S respectivly.

A simple example of the anular filter structure is the 2-port shown in Fig. 2e. Using the flowgraph method the S-matrix of this structure $s^R_{\nu\mu}$ can be obtained as a function of scattering parameters $s^T_{\nu\mu}$ of the T-junctions. For the transmission coefficient s^R_{12} the following expression can be given:

$$s^R_{12}=s^{T^2}_{12}.(EX_1+EX_2)(1-EX_1.EX_2(s^T_{22}-s^T_{23}))/NN \ ,$$

$$NN=1-s^{T^2}_{22}.(EX_1^2+EX_2^2)-2EX_1.EX_2.s^{T^2}_{23}- \qquad (3)$$
$$-(EX_1.EX_2)^2.(s^{T^2}_{22}+s^{T^2}_{23})^2 .$$

For $l_2=l_1$ (Fig. 2e) the above expression can be simplified to:

$$s^R_{12}=\frac{2EX_1.s^{T^2}_{12}}{1-EX_1^2(s^T_{22}+s^T_{23})^2} \ . \qquad (4)$$

This formula is not only simple, but allows a simple electromagnetic interpretation of the transmission zeros, as it is the subject of the reference[7].

It is easily seen from eq. (3), that in the case $l_2=l_1$ no transmission zero takes place, whereas in the case of $l_2\neq l_1$ two kinds of transmission zeros will appear at the frequencies:

$$f_1=\frac{(2k+1)Co}{\sqrt{\varepsilon_{eff}(f)}\ (l_2+l_1+2w_{1\ eff}(f))} \ , \qquad (5a)$$

$$f_2=\frac{(2k+1)Co}{2\sqrt{\varepsilon_{eff}(f)}\ (l_2-l_1)} \ , \text{ with } K=0,1,2,... \qquad (5b)$$

The first kind of transmission zeros, which will be occur, if $l_1+l_2+2w_{eff}(f)=(2k+1)\cdot\lambda$, are due to the ring resonances. The second kind of transmission zero, which will be appear, if $(l_2+w_{1eff}(f))-(l_1+w_{1eff}(f))=(2k+1)\lambda/2$, are caused by the interference of the waves traveling in opposite directions.

THEORETICAL AND EXPERIMENTAL RESULTS

Fig. 3 shows the theoretical and experimental behaviours of $|s_{21}|$ of two prototype microstrip structures as a low-pass and a band-stop filter versus the frequency in the range 0-7 GHz.

The theoretical results of isolation and insertion loss of the network filter between terminal 1 and each of the other three terminals are shown in Fig. 4. As it can be seen from Fig. 4 this circuit has one output with a relatively wide pass band and a second output with a sharp rejection band.

In Fig. 5 for different values of the modulus of the transmission coefficient $|s^R_{21}|$ of the anular 2-port structure isplotted against the frequency. While in the case of $\gamma = 100^o$ the two kinds of transmission zeros take place (Fig. 5a), in the case of $\gamma = 90^o$ only one kind of transmission zero can be observed (Fig. 5b). This is due to the fact that in the latter case the transmission zeros caused by the ring resonances coincide with those of interference of the waves traveling in opposite directions.

REFERENCES

1. R. Mehran, "The frequency-dependent scattering matrix of microstrip right-angle bends, T-junctions and crossings," Arch. Elek. Übertragung, vol. 29, pp. 454-460, Nov. 1975.
2. G. Kompa and R. Mehran, "Planar waveguide model for calculating microstrip components," Electron. lett., vol. 11, pp. 459-460, Sept. 1975.
3. G. Kompa, "S-matrix computation of microstrip discontinuities with a planar waveguide model," Arch. Elek. Übertragung, vol. 30, pp. 58-64, Feb. 1976.
4. W. Menzel and I. Wolff, "A method for calculating the frequency dependent properties of microstrip discontinuities," IEEE Trans. Microwave Theory Tech., vol. MTT-25, pp. 107-112, Feb. 1977.
5. R. Mehran, "The frequency-dependent scattering matrix of twofold truncated microstrip bends," Arch. Elek. Übertragung, vol. 31, pp. 411-415, Oct. 1977.
6. ——, "Calculation of microstrip bends and Y-junctions with arbitrary angle," IEEE Trans. Microwave Theory Tech., vol. MTT-26, June 1978.
7. G. D'inzeo, G. Giannini, R. Sorrentino and J. Vrba, "Microwave planar networks: The annular structure," Electron. Lett., vol. 14, pp. 526-528, August 1978.

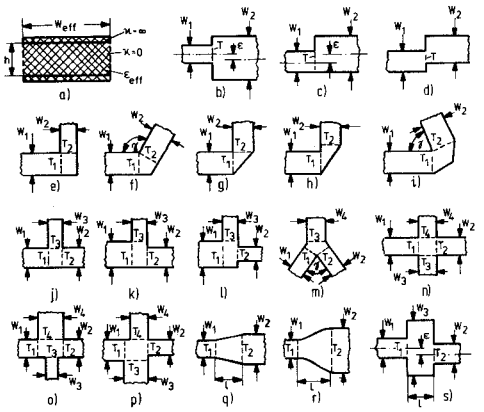

Fig. 1: Microstrip discontinuities.

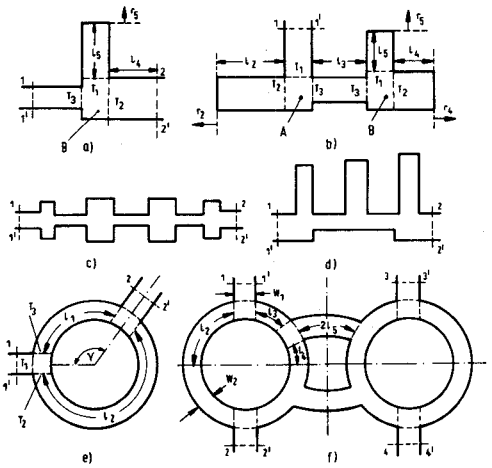

Fig. 2: Microstrip network filters.

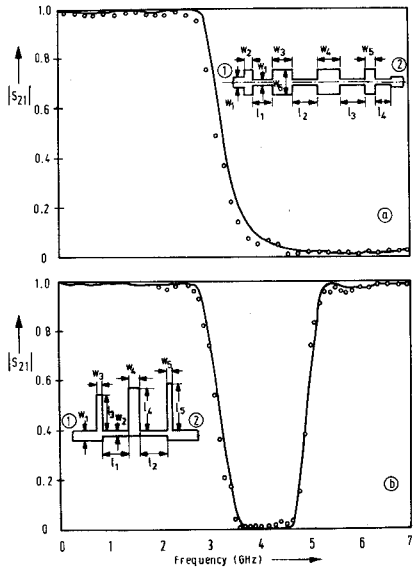

Fig. 3: Comparison between the theoretical (——) and experimental (ooo) results of $|s_{21}|$; ε_r=2.32,h=o.156cm.

a) chebyshev low-pass filter
b) Band-stop filter

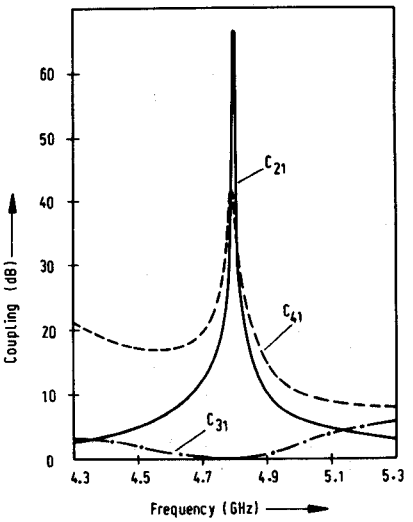

Fig. 4: Theoretical results of the coupling c_{v1} between terminal 1 and each of the other three terminals (Fig. 2f); ε_r=2.32,h=o.o794cm, w_1=o.23cm, w_2=o.13o2cm, l_2=1,8113cm,l_3=1.o127cm l_4=o.5115cm, l_5=o.5687cm.

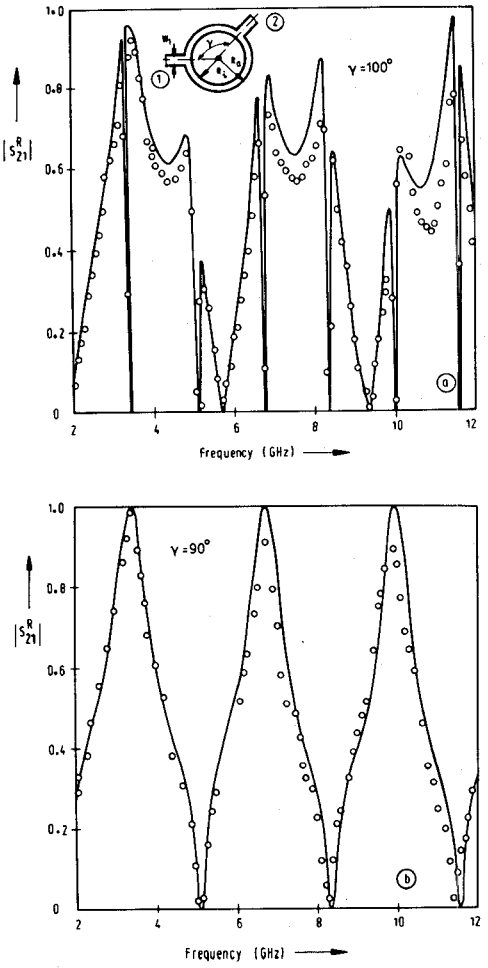

Fig. 5: Comparison between the theoretical (——) and experimental (ooo) results of $|s^R_{21}|$;ε_r=10.1, h=o.o635cm, w_1=o.o6cm, R_i=1cm,R_a=1.1cm.